

Composite high resolution localized relaxation scheme based on upwinding for hyperbolic conservation laws

Ritesh Kumar Dubey^{1,*},[†] and M. K. Kadalbajoo²

¹*Indian Institute of Information Technology, Jabalpur-482011, India*

²*Indian Institute of Technology, Kanpur 208016, India*

SUMMARY

In this work we present an upwind-based high resolution scheme using flux limiters. Based on the direction of flow we choose the smoothness parameter in such a way that it leads to a truly upwind scheme without losing total variation diminishing (TVD) property for hyperbolic linear systems where characteristic values can be of either *sign*. Here we present and justify the choice of smoothness parameters. The numerical flux function of a high resolution scheme is constructed using wave speed splitting so that it results into a scheme that truly respects the physical hyperbolicity property. Bounds are given for limiter functions to satisfy TVD property. The proposed scheme is extended for non-linear problems by using the framework of relaxation system that converts a non-linear conservation law into a system of linear convection equations with a non-linear source term. The characteristic speed of relaxation system is chosen locally on three point stencil of grid. This obtained relaxation system is solved using composite scheme technique, i.e. using a combination of proposed scheme with the conservative non-standard finite difference scheme. Presented numerical results show higher resolution near discontinuity without introducing spurious oscillations. Copyright © 2008 John Wiley & Sons, Ltd.

Received 8 February 2008; Revised 15 October 2008; Accepted 15 October 2008

KEY WORDS: hyperbolic conservation laws; TVD stability; high resolution schemes; relaxation model; composite schemes; non-standard finite difference methods

1. INTRODUCTION

Consider the 1D scalar conservation equation

$$\frac{\partial u}{\partial t} + \frac{\partial f(u)}{\partial x} = 0 \quad (1)$$

together with the initial condition

$$u(x, t=0) = u_0(x) \quad (2)$$

*Correspondence to: Ritesh Kumar Dubey, Indian Institute of Information Technology, Jabalpur-482011, India.

[†]E-mail: riteshkd@gmail.com, rkdshru@gmail.com

where $f(u)$ is a non-linear function of u . Numerical study and simulation of such problems are of great importance, as they often arise in the modeling of several physical phenomena in the area of computational fluid dynamics such as acoustics, aero-acoustics, weather prediction and ground water flows, etc. It has been seen that the classical numerical schemes for (1) either suffer from numerical dissipation or they are susceptible to numerical instabilities and exhibit spurious oscillations around points of discontinuity (sonic or extreme points) or in the region of steep gradients of the solution. In fact, even if the initial condition (2) is smooth, spurious oscillations get introduced by the higher-order schemes. Apart from the numerical instabilities, fundamental mechanical or thermodynamical principles can be violated.

In recent years, efforts have been made to build such schemes that can give high-order accuracy as well as be able to avoid such spurious oscillations [1–3]. Such high resolution schemes are conservative, generally (at most places) second-order accurate and non-oscillatory in nature and capable of resolving discontinuity in the solution [4, 5]. In [6, 7], a semi-discrete version of [2] is devised and its convergence to correct entropy satisfying solution is shown. Apart from the above flux limited methods, flux corrected transport methods are proposed in [8–10]. A semi-discrete essentially non-oscillatory class of schemes, based on polynomial reconstruction evolution, has been proposed in [11]. A good detail of the above methods can be found in [4, 5, 12, 13].

In [14], time marching dispersion relation preserving schemes are proposed. A non-dissipative numerical scheme for linear system is given in [15]. High resolution wave propagation algorithms based on solving Riemann problems for wave are given and implemented in [16, 17]. In [18], an arbitrary high-order finite volume scheme using derivatives (ADER) is proposed. In [19], efficient relaxation schemes are presented based on relaxation model [20] that replace the non-linear hyperbolic conservation law by a semi-linear system with a stiff relaxation term. In [21] relaxation schemes are presented as particular approximate Riemann solver. High-order WENO relaxation schemes are proposed in [22]. Recently, a non-standard finite difference method (NSFDM) introduced by Micken [23] is given in conservative form for Burger–Fisher equation [24]. More recently, a composite scheme using localized relaxation with NSFDM is given in [25].

In Section 2, we give some standard results and definitions used in the present work. In Section 3 construction of upwind-based high resolution scheme is given. In addition, the smoothness parameter is defined in such a way that it leads to a truly upwind scheme without losing total variation diminishing (TVD) property for negative convection speed or in general for hyperbolic linear systems where characteristic speed can be of either *sign*. Section 4 deals with the mathematical analysis of the scheme. The choice of limiter function is given in Section 5. Extension of the proposed scheme for non-linear problems by using relaxation model is given in Section 6. In Section 7, composite localized relaxation scheme is proposed. Numerical results are presented in Section 8 followed by the conclusion.

2. SOME RESULTS AND DEFINITIONS [5]

Definition 1

The conservative difference scheme for conservation law (1) is given by

$$U_i^{n+1} = U_i^n - \frac{\Delta t}{\Delta x} \{ \mathcal{H}_{i+1/2} - \mathcal{H}_{i-1/2} \} \quad (3)$$

where $\Delta t \mathcal{H}_{i\pm 1/2}$ approximate the flux of material across the sides $x = x_{i\pm 1/2}$ and $U_i^n \approx u(x_i, t^n)$. The approximate fluxes are written as

$$\begin{aligned}\mathcal{H}_{i+1/2}^n &= \mathcal{H}(U_{i-p}^n, \dots, U_{i+q}^n) \\ \mathcal{H}_{i-1/2}^n &= \mathcal{H}(U_{i-p-1}^n, \dots, U_{i+q-1}^n)\end{aligned}\quad (4)$$

The numerical flux functions $\mathcal{H}_{i\pm 1/2}$ depend on u at $p+q+1$ points.

Lemma 1

If $\mathcal{H}(u, u, \dots, u) = f(u)$, then the resulting conservative difference scheme (3) obtained by using the numerical flux function (4) will be consistent with conservation law (1) ([5, c.f. p. 157]).

Lemma 2

The truncation error of a conservative scheme of the form

$$U_i^{n+1} = \mathcal{Q}(U_{i-(p+1)}^n, \dots, U_{i+q}^n) \quad (5)$$

is given by

$$\tau_i^n = -\Delta t \left\{ \frac{\partial}{\partial x} \left(\xi(u) \frac{\partial u}{\partial x} \right) \right\}_{u=U_i^n} + \mathcal{O}(\Delta t^2 + \Delta x^2) \quad (6)$$

where $u = u(x, t)$ is a solution to conservation law (1) and

$$\xi(u) = \frac{1}{2} \left[\frac{1}{R^2} \sum_{j=-(p+1)}^q j^2 \mathcal{Q}_j(u, \dots, u) - [f'(u)]^2 \right] \quad (7)$$

where $R = \Delta t / \Delta x$ and \mathcal{Q}_j represents the partial derivative of \mathcal{Q} with respect to the $(p+2+j)$ th variable ([5, c.f. p. 184]).

Definition 2

A difference scheme is said to be TVD scheme if the numerical solution obtained by the scheme satisfies

$$\sum_{i=-\infty}^{\infty} |\Delta_+ U_i^{n+1}| \leq \sum_{i=-\infty}^{\infty} |\Delta_+ U_i^n| \quad \forall n \geq 0 \quad (8)$$

where $\Delta_+ U_i^n = U_{i+1}^n - U_i^n$.

3. HIGH RESOLUTION TVD SCHEME FOR LINEAR SYSTEMS

In this section we construct the numerical flux function of high resolution TVD scheme using flux limiters. Consider the following 1D linear hyperbolic system:

$$\frac{\partial \mathbf{U}}{\partial t} + \mathbf{A} \frac{\partial \mathbf{U}}{\partial x} = 0, \quad \mathbf{U}(x, 0) = U_0(x), \quad x \in \mathbb{R} \quad (9)$$

together with appropriate boundary conditions where $\mathbf{U} \in \mathbb{R}^m$ and $\mathbf{A} \in \mathbb{R}^m \times \mathbb{R}^m$. From the hyperbolicity, \mathbf{A} has m real eigenvalues $\lambda_p, p = 1, \dots, m$. Without loss of generality, system (9) can be

written as decoupled system of m scalar convection equations as

$$\frac{\partial W_p}{\partial t} + \lambda_p \frac{\partial W_p}{\partial x} = 0, \quad p = 1, \dots, m \tag{10}$$

where W_p is the the p th component of the characteristic variable $\mathbf{W} = \mathbf{K}^{-1}\mathbf{U}$ and λ_p is the p th eigenvalues of \mathbf{A} . Here \mathbf{K} is a matrix of eigenvectors of \mathbf{A} . The general solution of (9) in terms of original variable \mathbf{U} can be obtained by reverse transformation $\mathbf{U} = \mathbf{KW}$ ([12, c.f. 50–51]). Note that the eigenvalues λ_p of the linearly decoupled system (10) can be either positive or negative. Using wave splitting (10) can be written as

$$\frac{\partial W_p}{\partial t} + \left(\frac{\lambda_p + |\lambda_p|}{2}\right) \frac{\partial W_p}{\partial x} + \left(\frac{\lambda_p - |\lambda_p|}{2}\right) \frac{\partial W_p}{\partial x} = 0, \quad p = 1, \dots, m \tag{11}$$

Now, in view of the direction of flow we define the numerical flux of the scheme in such a way that it satisfies the physical hyperbolicity condition. Consider the numerical flux functions $\mathcal{H}_{l_{i+1/2}}$ and $\mathcal{H}_{h_{i+1/2}}$ of first-order and second-order upstream schemes, respectively, for the p th equation of system (10) (after dropping out the superscript for n th time level)

$$\mathcal{H}_{l_{i+1/2}} = \begin{cases} \lambda_p W_{p_i}, & \lambda_p > 0 \\ \lambda_p W_{p_{i+1}}, & \lambda_p < 0 \end{cases} \tag{12}$$

$$\mathcal{H}_{h_{i+1/2}} = \begin{cases} \frac{\lambda_p}{2}(3W_{p_i} - W_{p_{i-1}}), & \lambda_p > 0 \\ \frac{\lambda_p}{2}(3W_{p_{i+1}} - W_{p_{i+2}}), & \lambda_p < 0 \end{cases} \tag{13}$$

where $W_{p_i} \approx W_p(x_i)$ is the approximation of W_p at grid point x_i . We define the numerical flux function $\mathcal{H}_{p_{i+1/2}}$ of high resolution scheme for (11) as

$$\begin{aligned} \mathcal{H}_{p_{i+1/2}} &= \left(\frac{\lambda_p + |\lambda_p|}{2}\right) \left(W_{p_i} + \frac{\phi_{p_i}^+}{2}(W_{p_i} - W_{p_{i-1}})\right) \\ &+ \left(\frac{\lambda_p - |\lambda_p|}{2}\right) \left(W_{p_{i+1}} + \frac{\phi_{p_i}^-}{2}(W_{p_{i+1}} - W_{p_{i+2}})\right) \end{aligned} \tag{14}$$

The limiter function $\phi_{p_i}^\pm = \phi_{p_i}^\pm(\theta_{p_i}^\pm)$ needs to be defined in such a way that the numerical flux function $\mathcal{H}_{p_{i+1/2}}$ has smoothing capabilities of the first-order upwind scheme when it is necessary (i.e. near discontinuities) and the accuracy of the second-order upwind scheme (i.e. in the smooth region of solution) when it is possible. The smoothness parameter $\theta_{p_i}^\pm$ is a function of consecutive gradients. In order to achieve complete upwinding, depending on the sign of the eigenvalues λ_p , i.e. the direction of flow as shown in Figure 1, we define

$$\theta_{p_i}^+ = \frac{W_{p_i} - W_{p_{i-1}}}{W_{p_{i+1}} - W_{p_i}} \quad \text{and} \quad \theta_{p_i}^- = \frac{W_{p_{i+2}} - W_{p_{i+1}}}{W_{p_{i+1}} - W_{p_i}} \tag{15}$$

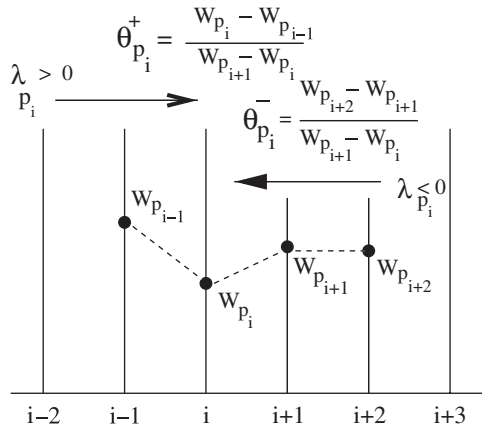


Figure 1. Definition of smoothness parameter depending on direction of flow.

Here, it is necessary to mention that the obvious choice to define $\theta_{p_i}^-$ for negative velocity seems to be

$$\theta_{p_i}^- = \frac{W_{p_{i+1}} - W_{p_i}}{W_{p_i} - W_{p_{i-1}}} = \frac{1}{\theta_{p_i}^+}$$

but it destroys the TVD property of the underlying scheme.

4. CONVERGENCE ANALYSIS

In this section we present TVD stability and accuracy of the proposed high resolution scheme.

Theorem 1

The conservative scheme obtained by using the flux function $\mathcal{H}_{p_{i+1/2}}$ is TVD under the constraint $0 \leq \phi_p^\pm \leq 2, 0 \leq \phi_p^\pm \leq 2/\theta_p^\pm$, when the CFL like condition

$$0 < \frac{\max |\lambda_p| \Delta t}{\Delta x} \leq \frac{1}{2}, \quad p = 1, \dots, m \tag{16}$$

is satisfied and the smoothness parameter is given by (15).

Proof

Let $\lambda_p < 0$, then by using numerical flux function (14) in (3), the resulting scheme can be written in incremental form as

$$W_{p_i}^{n+1} = W_{p_i} + \alpha_{i+1/2} \Delta_+ W_{p_i} - \beta_{i-1/2} \Delta_- W_{p_i} \tag{17}$$

where

$$\alpha_{i+1/2} = \left(C \frac{\phi_{p_i}^- \theta_i^-}{2} - C \left(1 + \frac{\phi_{p_{i-1}}^-}{2} \right) \right), \quad \beta_{i+1/2} = 0 \tag{18}$$

$C = \lambda_p \Delta t / \Delta x$ and $\Delta_+ W_{p_i} = W_{p_{i+1}} - W_{p_i} = \Delta_- W_{p_{i+1}}$. The necessary and sufficient condition for (17) to be TVD [1]

$$\alpha_{i+1/2} \geq 0, \quad \beta_{i+1/2} \geq 0 \quad \text{and} \quad 0 \leq \alpha_{i+1/2} + \beta_{i+1/2} \leq 1 \quad \forall i \tag{19}$$

Note that $\alpha_{i+1/2} \geq 0$ and $\beta_{i+1/2} \geq 0$; hence, TVD property requires

$$0 \leq \left(C \frac{\phi_{p_i}^- \theta_{p_{i+1}}^-}{2} - C \left(1 + \frac{\phi_{p_{i-1}}^-}{2} \right) \right) \leq 1 \quad \forall i \tag{20}$$

Since $C \in [-1/2, 0) \Rightarrow (1+C)/C \in [-1, -\infty)$ as $C \rightarrow 0^-$; therefore, solving (20) we have

$$|\phi_{p_i}^- \theta_{p_i}^- - \phi_{p_{i-1}}^-| \leq 2 \quad \forall i \tag{21}$$

Inequality (21) holds for

$$|\phi_{p_i}^- \theta_{p_i}^-| \leq 2 \quad \text{and} \quad |\phi_{p_{i-1}}^-| \leq 2 \quad \forall i \tag{22}$$

Dropping out the subscript i for space,

$$0 \leq \frac{\phi_p^-}{\theta_p^-} \leq 2 \quad \text{and} \quad 0 \leq \phi_p^- \leq 2 \tag{23}$$

Case 2: If $\lambda_p > 0$, similar analysis as the above can be done for the resulting scheme. This completes the proof. \square

Theorem 2

If the flux limiter ϕ_p^\pm is bounded, then the resulting difference scheme is consistent with the linear scalar equation (10). If $\phi_p^\pm(1) = 1$ and ϕ_p^\pm is Lipschitz continuous at $\theta_p^\pm = 1, \forall p = 1, \dots, m$ then the difference scheme is second-order accurate on smooth region of solution with $(W_p)_x$ bounded away from zero.

Proof

If $\lambda_p < 0$, consider the associated numerical flux of the scheme

$$\mathcal{H}_{p_{i+1/2}}(W_{p_i}, W_{p_{i+1}}, W_{p_{i+2}}) = \left(\frac{\lambda_p - |\lambda_p|}{2} \right) \left(W_{p_{i+1}} + \frac{\phi_{p_i}^-}{2} (W_{p_{i+1}} - W_{p_{i+2}}) \right) \tag{24}$$

Since $\phi_{p_i}^\pm$ is bounded, we have

$$\mathcal{H}_{p_{i+1/2}}(W_p, W_p, W_p) = \lambda_p W_p \tag{25}$$

The first claim follows from Lemma 1. We prove a slight variation of the second claim using the almost everywhere differentiability of Lipschitz continuous function. Rewrite the scheme as

$$\begin{aligned} W_{p_i}^{n+1} &= \mathcal{Q}(W_{p_{i-1}}, W_{p_i}, W_{p_{i+1}}, W_{p_{i+2}}) \\ &= \left(1 + C + \frac{C}{2} \right) W_{p_i} - \left(C + \frac{C}{2} \phi_{p_{i-1}}^- + \frac{C}{2} \phi_{p_i}^- \right) W_{p_{i+1}} + \frac{C}{2} \phi_{p_i}^- W_{p_{i+2}} \end{aligned} \tag{26}$$

In view of Lemma 2, here $p=0, q=2$. Note that ϕ_p^- is bounded and $\phi_{p_i}^-(1)=1$. At smooth region of solution $\theta_{p_i}^- = \theta_{p_{i-1}}^- = 1$. Therefore, in such region $\phi_{p_i}^{-'} = \phi_{p_{i-1}}^{-'} = 0$. Using the definitions for θ_i^\pm and above facts, one can show that

$$\sum_{j=-1}^2 j^2 \mathcal{Q}_j(W_p, \dots, W_p) = 0 \tag{27}$$

Using (6) and (7), one can deduce

$$\tau_i^n = -\Delta t \left\{ \left(-\frac{\lambda_p^2}{2} (W_p)_x \right)_x \right\}_{W_p=W_{p_i}^n} + \mathcal{O}(\Delta t^2 + \Delta x^2) \tag{28}$$

This shows that the resulting difference scheme is at least second-order accurate in the smooth region of the solution. Similarly, the result for $\lambda_p > 0$ can be shown. This completes the proof. □

5. CHOICE OF LIMITER FUNCTIONS

We need to maximize the limiter ϕ in order to minimize the diffusive effect of first-order flux $\mathcal{H}_{l_{i+1/2}}$ in $\mathcal{H}_{p_{i+1/2}}$ subject to the TVD constraints. An obvious choice is

$$\phi(\theta^\pm) = \min(2, 2/\theta^\pm), \quad \theta^\pm > 0$$

which is the upper limit of the TVD condition (23). Note that in order to make the resulting scheme second-order accurate whenever possible ϕ should be such that $\phi(1)=1$. This is also needed for Lipschitz continuity of $\phi(\theta)$ and required by Theorem 2 to guarantee the second-order accuracy away from extrema of solution. Based on the above requirements we choose the following limiters:

$$\phi_p(\theta_p) = \begin{cases} 0, & \theta_p \leq 0 \\ \min \left[2, \frac{2}{\theta_p}, \frac{1+\delta}{\delta+\theta_p} \right], & \theta_p > 0 \end{cases} \text{ for any fixed } \delta \in [0, \infty) \tag{29}$$

One can also use the following flux limiter function proposed in [26] for the given scheme:

$$\phi_p(\theta_p) = \begin{cases} 0, & \theta_p \leq 0 \\ \min \left[\frac{\theta_p + |\theta_p|}{(1 + |\theta_p|)}, \frac{1}{\theta_p} \right] & \text{otherwise} \end{cases} \tag{30}$$

Remarks

1. For every value $\theta > 0$ and any fixed $\delta \in [0, \infty)$, the above limiters are bounded, Lipschitz continuous and satisfy the condition $\phi(1)=1$, hence ensure the second-order of accuracy in the smooth region of solution. In addition, since this class of limiters satisfies the proposed TVD condition (23), therefore, yields TVD scheme.
2. Note that for linear problems a unique weak solution exists and Lax–Wendrof (LXW) theorem [27] along with the stability of the scheme guarantees the convergence of the scheme to the weak solution ([4, c.f. p. 129]).

6. LOCALIZED RELAXATION SCHEME: EXTENSION TO NON-LINEAR CASE

In this section we extend the proposed scheme for non-linear problems by using the framework of relaxation model that converts a non-linear conservation law into a system of linear convection equations with a non-linear source term. A splitting technique is used to solve the convection and source part of the relaxation system.

6.1. Relaxation system for hyperbolic equations

We apply the relaxation method [20] on the general 1D scalar conservation law (1) to obtain a relaxation system of the form

$$\begin{aligned}\frac{\partial u}{\partial t} + \frac{\partial v}{\partial x} &= 0 \\ \frac{\partial v}{\partial t} + \lambda^2 \frac{\partial u}{\partial x} &= -\frac{1}{\varepsilon}[v - f(u)]\end{aligned}\quad (31)$$

The initial conditions that lead to initial equilibrium and avoid the development of initial layer given by

$$u(x, t=0) = u_0(x), \quad v(x, t=0) = f(u_0(x)) \quad (32)$$

where v is a new variable, λ and the relaxation parameter $\varepsilon \ll 1$ are positive constants. For the small relaxation limit, one can obtain good approximation to the original conservation law (1) by solving relaxation system (31), i.e. for $\varepsilon \rightarrow 0^+$, the relaxation system can be approximated with leading order by

$$v = f(u) \quad (33)$$

$$\frac{\partial u}{\partial t} + \frac{\partial f(u)}{\partial x} = 0 \quad (34)$$

The state satisfying (33) is called the local equilibrium and (34) is the original conservation law (1). It is also shown in [20] that the relaxation system provides a vanishing viscosity model for the original conservation law (1) provided the characteristic value $f'(u)$ of (1) interlaces with λ as

$$-\lambda \leq f'(u) \leq \lambda \quad (35)$$

This important condition is called the sub-characteristic condition. The advantage in dealing with the relaxation system is that the convection terms are linear and the non-linear source term of (31) can be solved by using splitting method [20].

Remark

1. Since the relaxation system is linear; therefore, any consistent and stable numerical approximation in the zero relaxation limit are convergent and converges to the physically correct weak solution of the original conservation law (1) [20] (see Remark 2, Section 5).

6.2. Reduction to diagonal relaxation system

The relaxation system (31) for the scalar conservation law (1) can be written as

$$\frac{\partial \mathbf{U}}{\partial t} + \mathbf{A} \frac{\partial \mathbf{U}}{\partial x} = \mathbf{R} \quad (36)$$

where

$$\mathbf{U} = \begin{bmatrix} u \\ v \end{bmatrix}, \quad \mathbf{A} = \begin{bmatrix} 0 & 1 \\ \lambda^2 & 0 \end{bmatrix} \quad \text{and} \quad \mathbf{R} = \begin{bmatrix} 0 \\ -\frac{1}{\varepsilon}(v - f(u)) \end{bmatrix} \quad (37)$$

The system (36) can be diagonalized as $\mathbf{A} = \mathbf{BDB}^{-1}$. We transform the dependent variable $\mathbf{U}(x, t)$ by using the characteristic variable $\mathbf{W} = \mathbf{B}^{-1}\mathbf{U}$ to obtain the decoupled system as

$$\frac{\partial \mathbf{W}}{\partial t} + \mathbf{D} \frac{\partial \mathbf{W}}{\partial x} = -\frac{1}{\varepsilon}[\mathbf{W} - \mathbf{F}] \quad (38)$$

where

$$\mathbf{W} = \begin{bmatrix} w_1 \\ w_2 \end{bmatrix} = \begin{bmatrix} \frac{u}{2} - \frac{v}{2\lambda} \\ \frac{u}{2} + \frac{v}{2\lambda} \end{bmatrix}, \quad \mathbf{D} = \begin{bmatrix} -\lambda & 0 \\ 0 & \lambda \end{bmatrix} \quad \text{and} \quad \mathbf{F} = \begin{bmatrix} \frac{u}{2} - \frac{f(u)}{2\lambda} \\ \frac{u}{2} + \frac{f(u)}{2\lambda} \end{bmatrix} \quad (39)$$

For the above decoupled system (38), the initial condition (32) can be written as

$$u(x, t=0) = u_0(x), \quad \mathbf{W}(x, t=0) = \mathbf{F}(u_0(x)) \quad (40)$$

Note that the variables u and v can be obtained as

$$u = w_1 + w_2 \quad \text{and} \quad v = \lambda(w_2 - w_1) \quad (41)$$

In the small relaxation limit, i.e. $\varepsilon \rightarrow 0^+$ the decoupled system (38) is equivalent to the original conservation law (1). The decoupled system (38) can be solved by splitting it into two independently solvable steps, viz. convective and relaxation step. We write (38) as follows:

$$\frac{\partial \mathbf{W}}{\partial t} = \mathcal{S}^{(t)}(\mathbf{W}) + \mathcal{C}^{(t)} \quad (42)$$

where \mathcal{S} and \mathcal{C} represent the source and convection terms, respectively. One can solve (42) by a two step method as

$$\frac{d\mathbf{W}}{dt} = \frac{1}{\varepsilon}(\mathbf{F} - \mathbf{W}) \quad (43)$$

$$\frac{\partial \mathbf{W}}{\partial t} + \mathbf{D} \frac{\partial \mathbf{W}}{\partial x} = 0 \quad (44)$$

The relaxation step (43) can be solved by an implicit method; therefore, the time step is independent of the relaxation parameter ε . The solution of the relaxation step is given by

$$\mathbf{W} = (\mathbf{W}(t=0) - \mathbf{F})e^{-t/\varepsilon} + \mathbf{F} \quad (45)$$

Convection step (44) can be solved by the proposed upwind-based high resolution scheme in Section 3. Note that function \mathbf{F} does not change in the relaxation step as it is a function of u and $f(u)$; therefore, \mathbf{F} changes only in the convection step. To solve the convection step in relaxation system, we also define a parameter μ_i locally over the three point stencil of grid as in [25], i.e. $\mu_i = \max\{|f'(U_{i-1})|, |f'(U_i)|, |f'(U_{i+1})|\}$. We take the characteristic speeds of relaxation system (43)–(44) as $\lambda_j = (-1)^j \mu_i$, $j = 1, 2$. Thus, the relaxation system is solved locally by choosing the characteristic speed at each grid point. Note that the choice of λ_j 's satisfies the sub-characteristic condition $-\lambda \leq f'(u) \leq \lambda$. The application of high resolution scheme in Section 3 to the localized relaxation system yields a dissipative localized relaxation scheme because of inherent dissipative nature of the relaxation system (31) [28]. In the next section, we propose the use of a composite scheme technique to overcome the dissipative nature of the localized relaxation scheme.

7. COMPOSITE LOCALIZED RELAXATION SCHEME

In this section, we use the idea of composite scheme [29] in which a base-line numerical method is coupled with another numerical method having complementary features as a filter. Since the localized relaxation scheme is dissipative; therefore, to overcome this, we use Micken's less dissipative conservative NSFDM [24] as complementary scheme

$$\frac{U_i^{n+1} - U_i^n}{\Delta t} + \frac{1}{2} \left(\frac{(U_i^n)^2 - (U_{i-1}^n)^2}{\Delta x} \right) = 0 \quad (46)$$

for Burgers equation

$$\frac{\partial u}{\partial t} + \frac{\partial}{\partial x} \left(\frac{u^2}{2} \right) = 0 \quad (47)$$

Micken also gave a first-order non-conservative NSFDM for (47) in [23] as

$$\frac{U_i^{n+1} - U_i^n}{\Delta t} + U_i^{n+1} \left(\frac{U_i^n - U_{i-1}^n}{\Delta x} \right) = 0 \quad (48)$$

It has been seen (also shown in numerical results) that conservative NSFDM (46) captures the shock at right location but fails to capture the expansion fan with good accuracy (see Figure 8, Micken-C). In fact in the presence of sonic point (where the wave speed changes its sign) it completely fails and produces entropy violating solution (see Figure 9, Micken-C). These observations suggest to use the dissipative localized relaxation scheme in the presence of expansive sonic point in order to complement Micken's conservative scheme (46). Hence, in the region of smooth solution without sonic point, we propose to use Mickens' conservative NSFDM (47) to solve non-linear problems directly, otherwise, to use localized high resolution relaxation scheme as given in Section 6.2. It is done by using the proposed limiter function along with additional condition of positivity/negativity of wave speed at two consecutive grid points in space.

8. NUMERICAL RESULTS

Remarks

1. For all numerical computations, CFL condition is to be chosen as $C = (\Delta t / \Delta x) \mu \leq \frac{1}{2}$, where $\mu = \max\{\mu_i, \forall i\}$. Note that it is the CFL condition for the second-order upwind scheme for convection equation, hence also for the high resolution scheme proposed in Section 3 and 4.
2. For computation we choose the relaxation parameter $\varepsilon = 10^{-8}$ as suggested in [20].

8.1. 1D linearized equation of gas dynamics

Consider the following 1D linearized equations of gas dynamics:

$$\begin{aligned} \frac{\partial \rho}{\partial t} + \rho_0 \frac{\partial u}{\partial x} &= 0 \\ \frac{\partial u}{\partial t} + \frac{a}{\rho_0} \frac{\partial \rho}{\partial x} &= 0, \quad x \in [-2, 2], \quad t > 0 \end{aligned} \quad (49)$$

with the initial condition

$$\rho(x, 0) = \begin{cases} 2, & x > 0 \\ \frac{1}{2}, & x < 0 \end{cases} \quad \text{and} \quad u(x, 0) = 0 \quad \forall x \in [-2, 2] \quad (50)$$

and constant boundary conditions. Here $\rho(x, t)$ and $u(x, t)$ are density and speed, respectively, ρ_0 is the reference density and $a > 0$ is the sound speed. Computed results are given at time $t = 1$, $\Delta x = 0.02$, for $\rho_0 = a = 1$ in Figures 2–5.

Graphs are given for first-order upwind (1st_up), second-order upwind (2nd_up), LxW, Sweby's scheme using van Leer (SwebyV) and Min-mod (SwebyM) limiters along with the proposed high resolution scheme using flux limiters (29) corresponding to $\delta = 1$ and $\delta = 9$. Computed solution is compared with exact solution (exsol). A comparison is given between Sweby's scheme (using min-mod limiter) with the proposed scheme corresponding to $\delta = 1$ in lowest right-most graph in Figures 2 and 3. Comparison clearly shows that the proposed scheme gives higher resolution near discontinuity as compared with Sweby's scheme without introducing spurious oscillations. In Figure 6, numerical results are given by using definition $\theta_{p_i}^- = 1/\theta_{p_i}^+$, which show that spurious oscillations get introduced and leads to non-TVD solution.

8.2. Non-linear scalar problem

We take non-linear problem as inviscid Burgers equation given by

$$\frac{\partial u}{\partial t} + \frac{\partial}{\partial x} \left(\frac{u^2}{2} \right) = 0, \quad t > 0 \quad (51)$$

with periodic boundary conditions. It is well known that inviscid Burgers equation governs simple acoustic waves and hence allows shocks [12]. We present three different test cases to show the accuracy and high resolution shock capturing ability of proposed composite scheme.

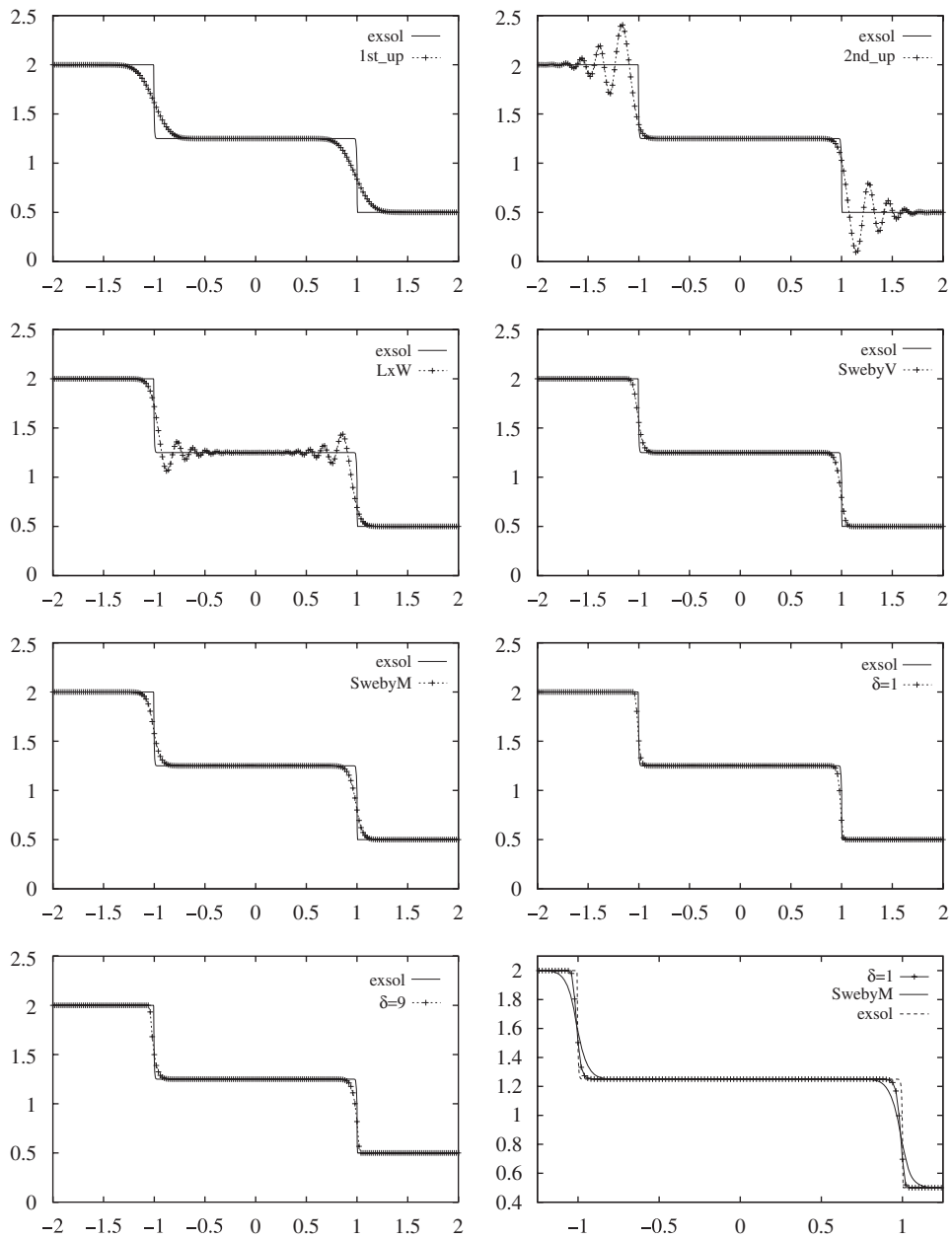


Figure 2. Density: comparison of numerical results using $C=0.2$.

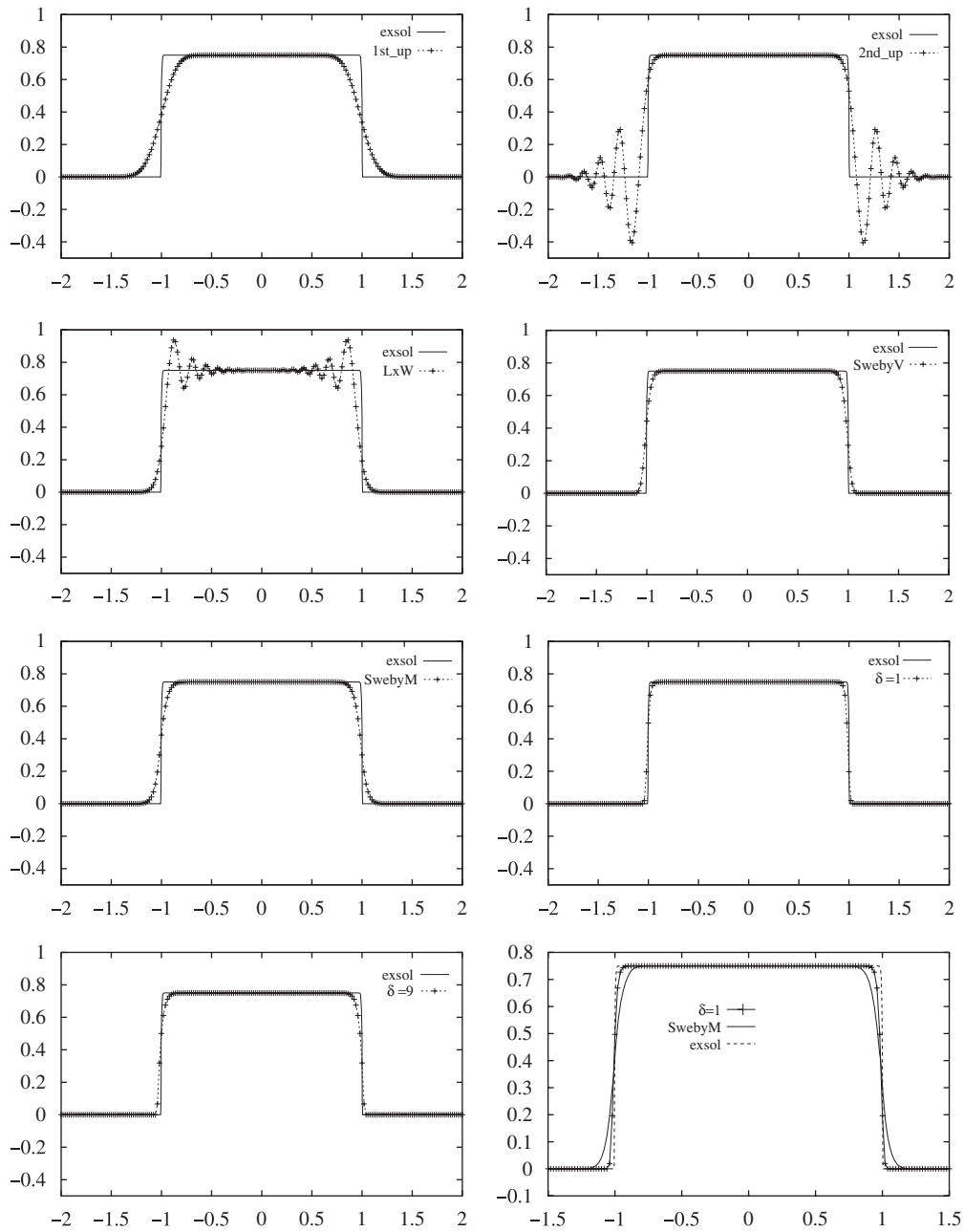


Figure 3. Velocity: comparison of numerical results using $C=0.2$.

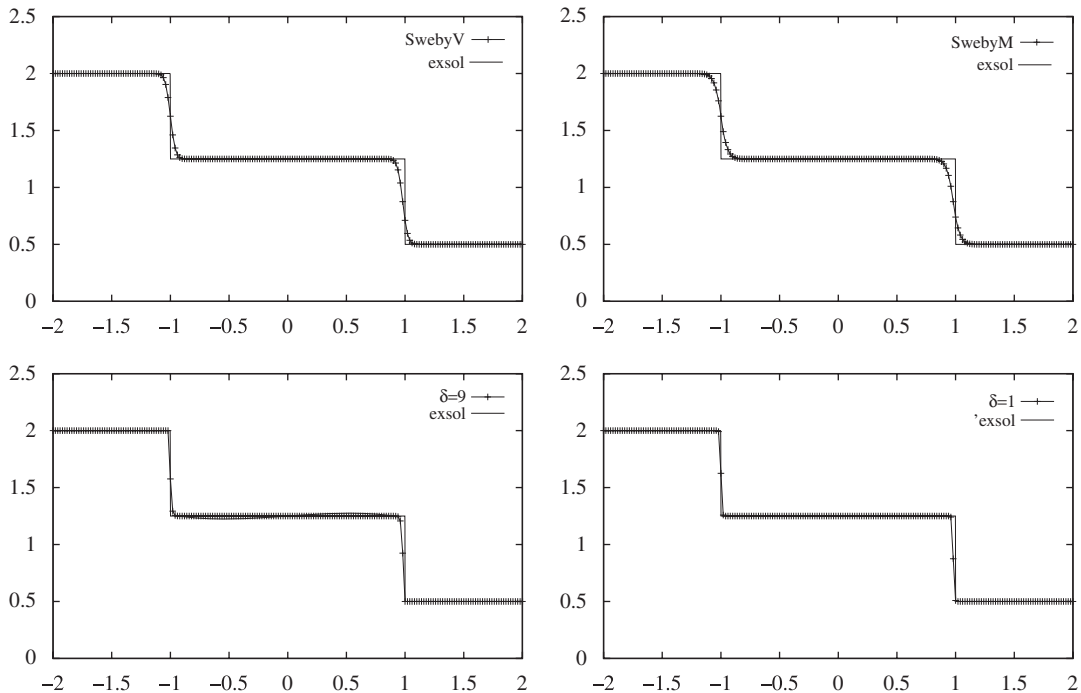


Figure 4. Density: comparison of numerical results using $C=0.5$.

8.2.1. *Case 1: accuracy test for pre- and post- shock solutions.* In this example, we take smooth sinusoidal initial condition as

$$u(x, 0) = -\tau \sin(x), \quad x \in [0, 2\pi] \tag{52}$$

It is a consequence of nonlinearity of (51) that the (non-trivial) solution beginning from smooth initial conditions will eventually develop a finite-time derivative singularity. An exact Fourier sine series solution for this problem is given by Platzman in [30].

$$u(x, t) = -2 \sum_{n=1}^{\infty} \frac{J_n(\tau nt)}{nt} \sin(nx) \tag{53}$$

where J_n is the Bessel function. This Fourier representation is valid prior to wave breaking time $t_b = 1$. Table I demonstrates L^1 and L^∞ -norms of the errors of proposed composite high resolution localized relaxation scheme (CHRLRS) and Lax–Friedrich’s (LxF) scheme at pre-shock time $t=0.3$ when the solution is still smooth. In Figure 7, approximate solutions are presented at the post-shock time $t=2.0$ when the shock is well developed. The graph shows that the proposed composite scheme (CHRLRS) captures the shock at right location with higher accuracy. In Table I error reduction due to doubling of the number of grid points is comparable with LXF scheme, in fact, point wise errors by CHRLRS are significantly smaller than the LxF scheme. It shows the first-order accuracy of the proposed composite scheme, which is well supported as Micken’s conservative scheme is only first-order accurate.

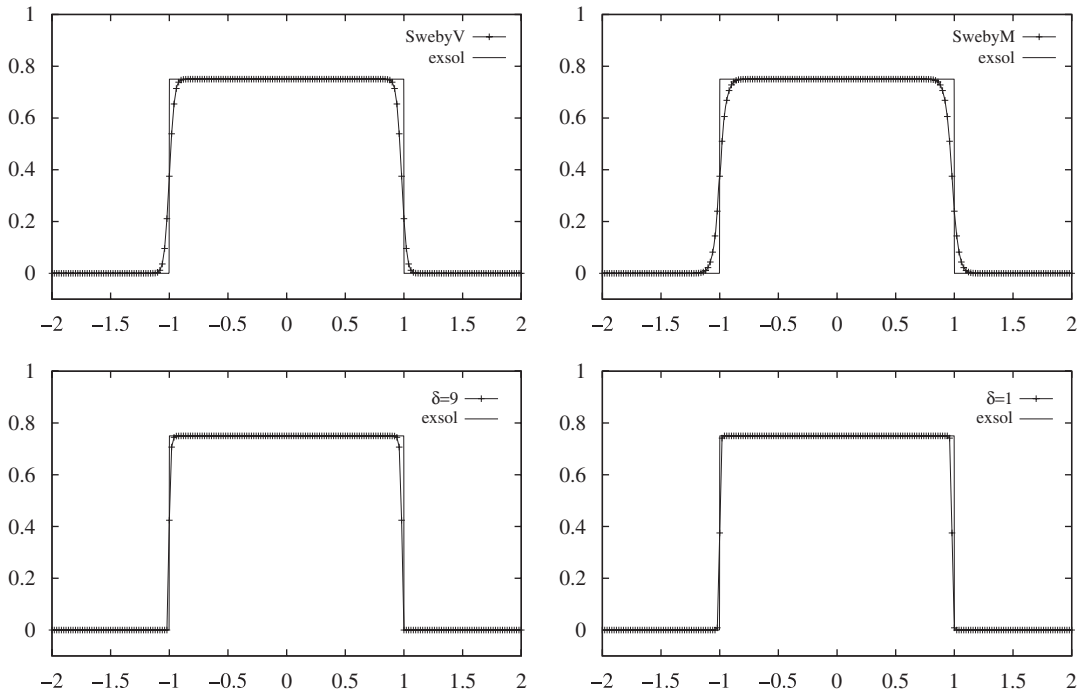


Figure 5. Velocity: comparison of numerical results using $C=0.5$.

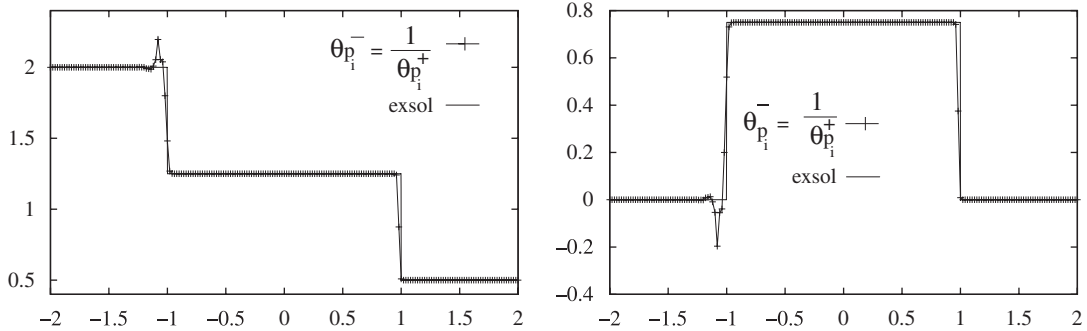


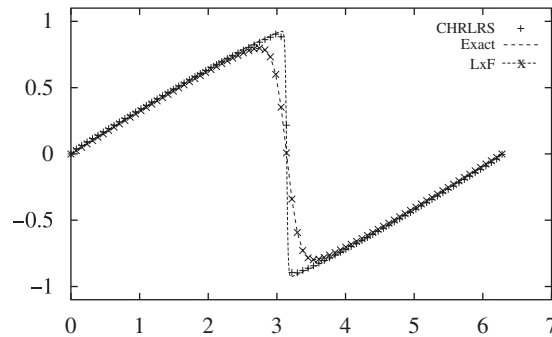
Figure 6. Non-TVD solution.

8.2.2. *Case 2: shock and simple expansion fan.* Here we consider the Burgers equation (51) along with the following initial condition:

$$u(x, 0) = \begin{cases} 1 & \text{for } |x| < \frac{1}{3} \\ 0 & \text{for } |x| > \frac{1}{3} \end{cases} \quad (54)$$

Table I. Solution error behavior with the mesh refinement.

N	CHRLRS				LxF			
	L^1 -norm	Rate	L^∞ -norm	Rate	L^1 -norm	Rate	L^∞ -norm	Rate
10	0.03422		0.0683		0.19255		0.3506	
20	0.01677	2.04	0.0347	1.96	0.11038	1.74	0.1937	1.81
40	0.01054	1.59	0.0312	1.11	0.05969	1.84	0.1003	1.93
80	0.00701	1.50	0.0204	1.53	0.03115	1.89	0.0493	2.03
160	0.00321	2.18	0.0098	2.08	0.01562	1.99	0.0255	1.93
320	0.00196	1.63	0.0052	1.88	0.00795	1.96	0.0119	2.14

Figure 7. Comparison of numerical solutions for $C=0.5$, $N=80$.

This test case has no sonic point in its solution. In it jumps at $x=-\frac{1}{3}$ and $x=\frac{1}{3}$ create a simple expansion fan and a strong steady right shock, respectively. In Figure 8, the exact solution is compared with Micken's non-conservative NSFDM (Micken-NC), conservative NSFDM (Micken-C), Roe's first-order upwind method with Harten's entropy fix (Harten), LxF, composite localized relaxation (CLR) scheme proposed in [25] and with the proposed CHRLRS. The limiter function (30) is used for CHRLRS. Results in Figure 8 show that the proposed CHRLRS captures the left expansion fan and strong steady shock with high accuracy and produces better results than other methods.

8.2.3. Case 3: Shock and expansion wave capturing in presence of expansive sonic point. Consider the Burgers equation (51) with the following initial condition:

$$u(x, 0) = \begin{cases} 1 & \text{for } |x| < \frac{1}{3} \\ -1 & \text{for } |x| > \frac{1}{3} \end{cases} \quad (55)$$

In this case, the jump at $x=-\frac{1}{3}$ creates a simple centered expansion fan and the jump at $x=\frac{1}{3}$ creates a shock. The unique sonic point is zero [12] and the wave speed $f'(u)$ changes sign from

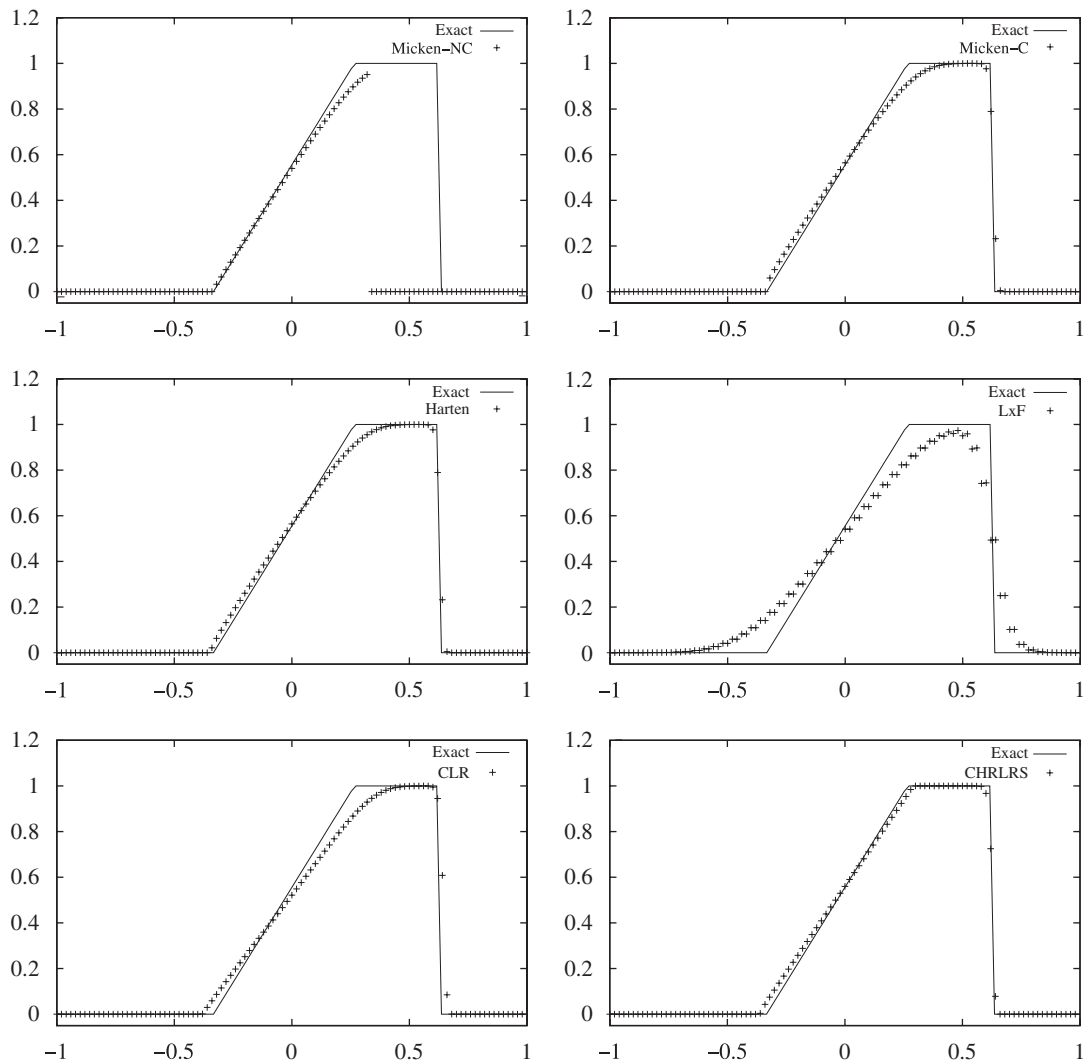


Figure 8. Comparison of numerical results using $C=0.5$, $\Delta x=0.02$ at time $t=0.6$.

–1 to 1. Computed solutions of proposed high resolution localized relaxation scheme (HRLRS), CHRLRS and other numerical methods are presented in Figures 9 and 10.

The results in Figure 9 show that Micken's non-conservative NSFDM (Micken-NC) and conservative NSFDM (Micken-C) both fail to capture the expansion fan with sonic point. Roe's first-order upwind method with Harten's entropy fix (Harten), LxF and CLR scheme proposed in [25] capture shock wave and expansion fan but overly diffusive as compared with the proposed composite scheme (CHRLRS). The proposed composite scheme (CHRLRS) captures the shock at right location and expansive waves with higher accuracy.

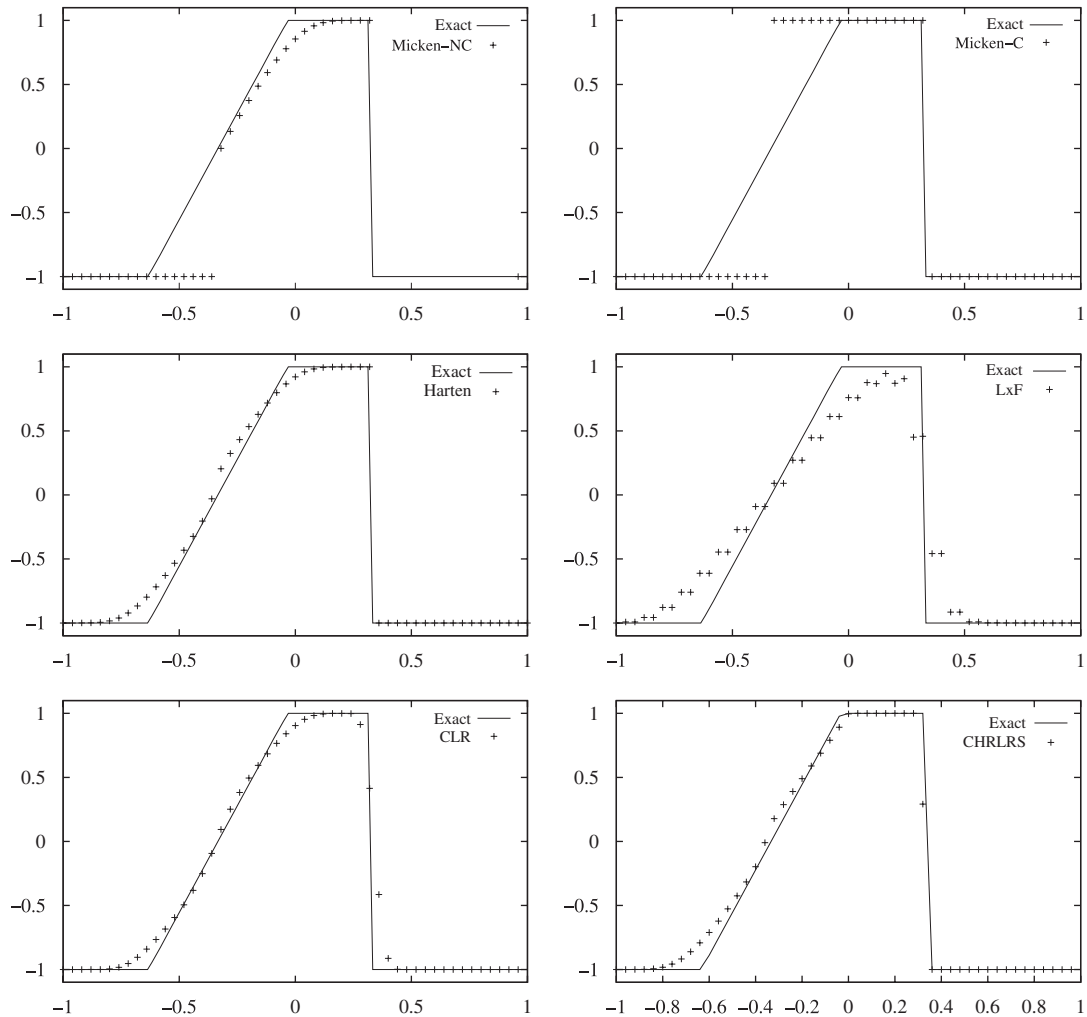


Figure 9. Comparison of numerical results using $C=0.5$, $\Delta x=0.04$ at time $t=0.3$.

In Figure 10, the results are also given by proposed HRLRS. The graphs show that the proposed scheme (CHRLRS) produces accurate solutions at the shock and gives better resolution at the head and tail of expansion wave as compared with other schemes.

Remarks

- In case of linearized equations of gas dynamics, graphs are given only for limiter function (29) corresponding to $\delta=1$ and $\delta=9$. Comparable results are obtained for other values of δ .
- For Burgers equation, graphs are given only for the limiter function (30), though comparable results are obtained by limiters (29).

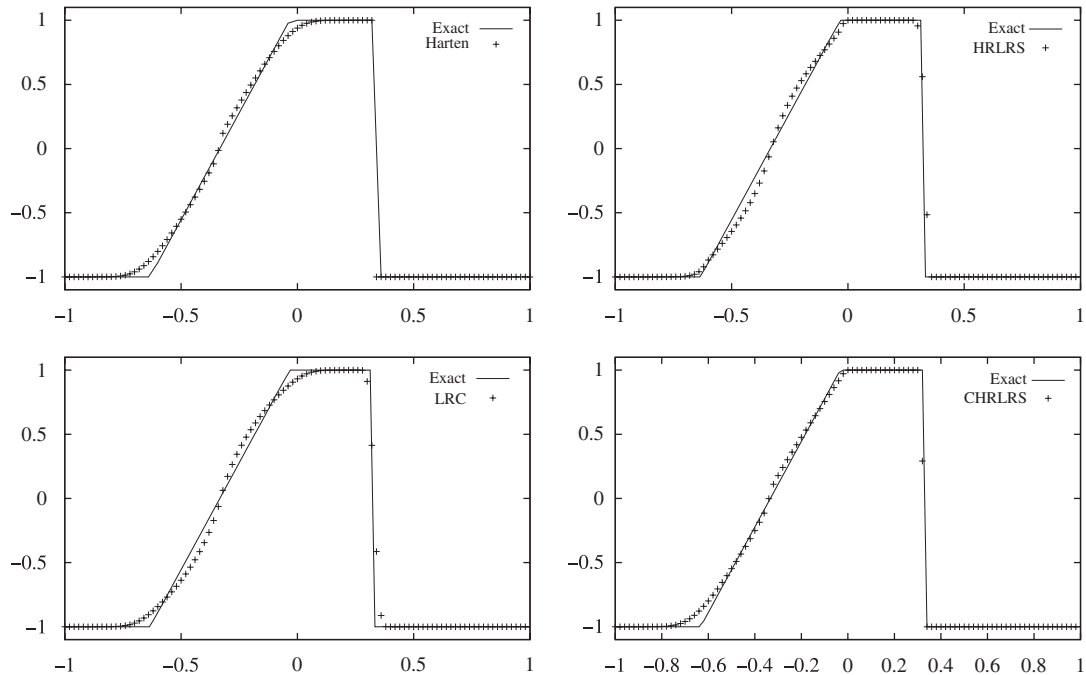


Figure 10. Comparison of numerical results using $C = 0.4$, $\Delta x = 0.02$ at time $t = 0.3$.

9. CONCLUSION AND FUTURE WORK

A truly upwind-based high resolution TVD scheme using flux limiter for linear system of hyperbolic conservation laws is presented. The choice of smoothness parameter is given and justified for negative characteristic values. The construction of the scheme and TVD bounds is given for the flux limiter function. Extension for the non-linear scalar case is done by using a relaxation model. This relaxation system is solved by splitting and choosing the eigen values of relaxation system locally at each grid point. Composite scheme technique is used to overcome the dissipative nature of the obtained relaxation scheme by using the non-standard finite difference scheme of Micken. Numerical results are given for linear and non-linear test problems, which show high resolution in the vicinity of discontinuity as compared with other benchmark schemes. Extension of the proposed scheme for non-linear system is under investigation.

REFERENCES

1. Harten A. High resolution schemes for conservation laws. *Journal of Computational Physics* 1983; **49**:357–393.
2. Sweby PK. High resolution schemes using flux limiters for hyperbolic conservation laws. *SIAM Journal on Numerical Analysis* 1984; **21**:995–1010.
3. van Leer B. Towards the ultimate conservative scheme, II. Monotonicity and conservation combined in a second order scheme. *Journal of Computational Physics* 1974; **14**:361–370.
4. Leveque RJ. *Numerical Methods for Conservation Laws*. Lectures in Mathematics. Birkhauser: ETH Zurich, 1999.

5. Thomas JW. *Numerical Partial Differential Equations, Conservation Laws and Elliptic Equations*. Text in Applied Mathematics, vol. 33. Springer: Berlin, 1999.
6. Osher S, Chakravarthy S. High resolution schemes and entropy conditions. *SIAM Journal on Numerical Analysis* 1984; **21**:955–984.
7. Osher S, Chakravarthy S. *Very High Order Accurate TVD Schemes, Oscillation Theory, Computation, and Methods of Compensated Compactness*. The IMA Volumes in Mathematics and its Applications, vol. 2. Springer-Verlag, 1986.
8. Boris JP, Book DL. Flux corrected transport I. SHASTA, a fluid transport algorithm that works. *Journal of Computational Physics* 1973; **11**:38–69.
9. Boris JP, Hain K. Flux corrected transport II. Generalization of the method. *Journal of Computational Physics* 1975; **18**:248–283.
10. Zalesak ST. Fully multidimensional flux corrected transport algorithms for fluids. *Journal of Computational Physics* 1979; **31**:335–362.
11. Shu CW, Osher S. Efficient implementation of essentially non-oscillatory shock capturing schemes. *Journal of Computational Physics* 1988; **77**:439–471.
12. Laney CB. *Computational Gas-dynamics* (1st edn). Cambridge University Press: Cambridge, 1998.
13. Toro EF. *Riemann Solvers and Numerical Methods for Fluid Dynamics, A Practical Introduction* (2nd edn). Springer: Berlin, 1999.
14. Tam CKW, Webb JC. Dispersion-relation-preserving finite difference schemes for computational acoustics. *Journal of Computational Physics* 1993; **107**:262–281.
15. Thomas JP, Roe PL. Development of non-dissipative numerical schemes for computational aero-acoustics. *AIAA Paper 93-3382*, July 1993.
16. Fogarty TR, Leveque RJ. High-resolution finite volume methods for acoustic waves in periodic and random media. *Journal of the Acoustical Society of America* 1999; **106**:17–28.
17. Leveque RJ. Wave propagation algorithms for multidimensional hyperbolic systems. *Journal of Computational Physics* 1997; **131**:327–353.
18. Schwartzkopff T, Munz CD, Toro EF. ADER: A high order approach for linear hyperbolic systems in 2D. *Journal on Scientific Computing* 2002; **17**:231–240.
19. Kumar R, Kadalbajoo MK. Efficient second order relaxation schemes for hyperbolic systems of conservation laws. *International Journal for Numerical Methods in Fluids* 2007; **55**:483–507.
20. Jin S, Xin Z. The relaxation schemes for systems of conservation laws in arbitrary space dimensions. *Communications in Pure and Applied Mathematics* 1995; **48**:235–276.
21. Leveque RJ, Pelanti M. A class of approximate Riemann solvers and their relation to relaxation schemes. *Journal of Computational Physics* 2001; **172**:572–591.
22. Banda MK, Seaid M. Relaxation WENO schemes for multidimensional hyperbolic systems of conservation laws. *Numerical Methods for Partial Differential Equations* 2007; **23**:1211–1334.
23. Micken RE. *Non-standard Finite Difference Models of Differential Equations*. World Scientific: Singapore, 1994.
24. Micken RE. Construction and analysis of a non-standard finite difference scheme for Burgers–fisher equations. *Journal of Sound and Vibration* 2002; **257**:791–797.
25. Kumar V, Raghurama Rao SV. Composite scheme using localized relaxation with non-standard finite difference method for hyperbolic conservation laws. *Journal of Sound and Vibration* 2007; DOI: 10.1016/j.jsv.2007.09.055.
26. Kumar R, Kadalbajoo MK. A class of high resolution shock capturing schemes for hyperbolic conservation laws. *Applied Mathematics and Computation* 2008; **195**:110–126.
27. Lax PD, Wendroff B. Systems of conservation laws. *Communications in Pure and Applied Mathematics* 1969; **13**:217–237.
28. Natalini R. *Recent Mathematical Results on Hyperbolic Relaxation Problems, Analysis of Systems of Conservation Laws*. Pitman Research Notes in Mathematics Series. Longman: Harlow, 1988.
29. Liska R, Wendroff B. Composite schemes for conservation laws. *SIAM Journal on Numerical Analysis* 1998; **35**:2250–2271.
30. Platzman GW. An exact integral of complete spectral equations for unsteady one dimensional flow. *Tellus* 1964; **XVI**:422–431.